J Mater Sci: Mater Electron (2014) 25:3160–3165
DOI 10.1007/s10854-014-1998-8

# Chemical bath deposition of SnS thin films on ZnS and CdS substrates

**M. Safonova · P. K. Nair · E. Mellikov · A. R. Garcia · K. Kerm · N. Revathi · T. Romann · V. Mikli · O. Volobujeva**

Received: 6 March 2014 / Accepted: 8 May 2014 / Published online: 15 May 2014


**Abstract** We illustrate that Tin sulfide (SnS) thin films of 110–500 nm in thickness may be deposited on ZnS and CdS substrates to simulate the requirement in developing window-buffer/SnS solar cells in the superstrate configuration. In the chemical bath deposition reported here, tin chloride and thiosulfate are the major constituents and the deposition is made at 25 °C. In a single deposition, film thickness of 110–170 nm is achieved and in two more successive depositions, the film thickness is 450–500 nm. The thicker films are composed of vertically stacked flakes, 100 nm across and 10–20 nm in thickness. The Sn/S elemental ratio is ~1 for the films 110–170 nm in thickness, but it slightly increases for thicker films. The crystalline structure is orthorhombic, similar to the mineral herzenbergite, and with crystallite diameters 13 nm (110–170 films) and 16 nm (450–500 nm films). The Raman bands at 94, 172 and 218 $cm^{-1}$ further confirm the SnS composition of the films. The optical band gap of SnS is 1.4–1.5 eV for the thinner films, but is 1.28–1.39 eV for the thicker films, the decrease being ascribed to the increase in the crystallite diameter. Uniform pin-hole free SnS thin films were successfully grown on two different substrates and can be applied in solar cell structures.

M. Safonova (✉) · E. Mellikov · K. Kerm · N. Revathi · V. Mikli · O. Volobujeva
Department of Materials Science, Tallinn Technical University, Ehitajate tee 5, 19086 Tallinn, Estonia
e-mail: marija.safonova@gmail.com

P. K. Nair · A. R. Garcia
Department of Solar Energy Materials, Instituto de Investigación en Energía, Universidad Nacional Autónoma de México, 62580 Temixco, Morelos, Mexico

T. Romann
Institute of Chemistry, University of Tartu, Ülikooli 18, 50090 Tartu, Estonia

## 1 Introduction

Tin sulfide (SnS) is one of the most promising materials for low-cost thin film solar cells, since its band gap (1.3–1.4 eV) is near to the optimum value of 1.3–1.5 eV for solar cell and its absorption coefficient is appreciably high in the visible region (>$10^4$ $cm^{-1}$). In addition, the elemental constituents of this material are nontoxic and abundant in nature [1].

For the deposition of thin films of SnS various methods like thermal evaporation, pulse electrodeposition, spray pyrolysis, SILAR, electron beam evaporation, chemical bath deposition (CBD) have been employed [2]. Among these methods CBD is relatively simple, and inexpensive method suitable for deposition at low temperature on large substrates irrespective of the shape and morphology of substrates [3]. However, CBD is a complicated process. There are many parameters which influence the deposition of SnS films, such as atmosphere medium, ion concentration, defect chemistry, aqueous medium of the bath solution, temperature [4] and substrate nature.

Recently, a record efficiency SnS solar cell of 1.95 % (active area) was fabricated from p–n homojunction nanowires using boron and phosphorus as dopants. In addition, SnS-based solar cells have been reported using different n-type partners such as ZnO, CdS, $Cd_{1-x}Zn_xS$. So far, the best SnS planar heterojunction device was fabricated with SnS/CdS, achieving power conversion efficiency (η) of 1.3 % [5]. However, there are some concerns that CdS can have harmful effects on the kidneys and bone.

On the other hand, ZnS is very suitable for a window layer of heterojunction solar cells [6].

The aim of this work was to investigate properties of SnS films depending on the substrate materials and number (1–3) of sequential deposition. Films were deposited on ZnS and CdS substrates, because they suit well as buffer layers for solar cells with SnS absorber layer. One, two and three times deposited SnS films were prepared. The structural, morphological, optical and electrical properties of these films were investigated.

## 2 Experimental

### 2.1 Deposition of ZnS films

ZnS thin films were prepared by CBD technique, consecutively stirring zinc sulfate, triethanolamine, ammonium hydroxide, thioacetamide with respective molar concentrations of 0.025, 0.014 M, concentrated, 0.01 M in total volume [7]. Deionized water was added to obtain total solution volume of 100 ml. Corning glass substrates, which were previously washed with detergent, were placed vertically in solution. Deposition was held at room temperature for 24 h. Obtained films were washed with cotton and rinsed with deionized water, then dried. Films were heated in the air for 15 min at 270 °C to obtain good adherence of consecutively deposited SnS film.

### 2.2 Deposition of CdS films

CdS thin films were prepared by CBD, consecutively stirring cadmium nitrate, sodium citrate, ammonium hydroxide and thiourea solutions with respective molar concentrations of 0.025, 0.15 M, concentrated, 0.05 M in total volume [8]. Deionized water was added to obtain total solution volume of 100 ml. Corning glass substrates, which were previously washed with detergent and then in ultrasonic bath with acetone, were placed vertically in solution. Deposition was held at 80 °C during 1 h and 30 min. Obtained films were washed using cotton and rinsed with deionized water, then dried.

### 2.3 Deposition of SnS films

SnS thin films were prepared by CBD. Few drops of hydrochloric acid were added to stannous chloride to dissolve it, molar concentration of stannous chloride in total volume is 0.03 M. Next, tartaric acid was added with molar concentration in total volume of 0.44 M. Deionized water was added and then ammonium hydroxide to obtain the pH of solution equal to 7. The last component added was sodium thiosulphate with molar concentration in total volume of 100 ml 0.03 M [9]. Corning glass substrates with previously deposited CdS or ZnS thin films were placed vertically in solution. Deposition was held at room temperature during 24 h. Obtained films were washed and rinsed with deionized water, then dried. Consecutive depositions of two and three times were made additionally to obtain thicker films. Deposition made directly on glass substrates lacks the good quality obtainable on CdS or ZnS substrate layers.

### 2.4 Characterization of films

XP Plus Stylus Profilometer was used to determine thickness of the films. X-ray diffraction analyse was made to evaluate crystalline structure of films, using Rigaku Ultima IV X-ray diffractometer using Cu-K$\alpha$ radiation with 2$\theta$ ranging from 10° to 70°. Scanning electron microscope (SEM) Hitachi SUI 510 and HR-SEM Zeiss ULTRA 55 images were taken to obtain information on films surface morphology and attached EDAX Oxford x-act analyser to determine the elemental composition of the films. The optical transmittance and near-normal specular reflectance of the films were recorded using a Shimadzu UV–VIS–NIR scanning spectrophotometer in the wavelength range of 250–2,500 nm. Electrical characteristics were measured using Keithley 619 electrometer with Keithley 230 programmable voltage source. Hall-effect measurements were done at room temperature using an MMR Technologies H-50 unit, allowing for the determination of charge-carrier type. Raman spectral measurements were made at room temperature on a high resolution micro-Raman spectrometer (Horiba JobinYvon HR800) equipped with a multichannel CCD detection system in the backscattering configuration. An Nd-YAG laser ($\lambda = 532$ nm) with a spot size of 10 μm in diameter was used for excitation. Bruker Multimode 8 Atomic Force Microscope (AFM) with nanoscope V controller was used to determine roughness of the films surface.

## 3 Results and discussion

### 3.1 Thickness

Film thickness in series CdS/SnS found to be slightly higher (173 nm for one-time and 505 nm for three-times deposition) than that in the ZnS/SnS series (114 nm for one-time and 455 nm for three-times deposition). Whether this is due to dissolution of the ZnS substrate layer is not clear.

**Table 1** Changes in composition of SnS thin films of series ZnS/SnS and series CdS/SnS in multiple deposition process

| Series | Sn atomic % | S atomic % |
|---|---|---|
| ZnS/SnS | | |
| X1 | 50.95 | 48.04 |
| X2 | 53.44 | 46.56 |
| X3 | 56.09 | 43.60 |
| CdS/SnS | | |
| X1 | 50.18 | 49.82 |
| X2 | 50.20 | 49.80 |
| X3 | 50.69 | 49.31 |

### 3.2 Elemental analyses and surface morphology

Table 1 shows atomic ratios of tin and sulphur in as-deposited films of series ZnS/SnS and CdS/SnS. In series CdS/SnS in multiple deposition process the ratio of tin to sulphur is almost 1:1, which means, that these films were in a nearly stoichiometric composition of stannous monosulphide. The films deposited on ZnS substrate were stoichiometric only after single CBD, but tin-rich in multiple deposition series, with a continuous increase of concentration of tin in films. The similar increase of Sn concentration in SnS films by CBD deposition process was reported by Patel [10]. At the same time, Raman investigations did not indicate the existence of any additional to SnS phases in CBD films on ZnS substrate.

Figures 1 and 2 show SEM images of SnS films of the CdS/SnS and ZnS/SnS series. Images indicate uniform pinhole free surface of the SnS thin films on both substrates. The images also show complete, continuous and uniform coverage of material over the surface of the films. The films of similar thickness on CdS and ZnS substrates demonstrate slightly different morphology, but in general they consist of vertically stacked flake structures, of about 100–150 nm laterally and of thickness of around 20 nm. The film morphology reported here is similar to those obtained by Wang et al. [11]. The absence of particulate precipitate in both cases indicates that the dominating deposition mechanism of the films on ZnS substrate may be ion-by-ion mechanism [3]. The surface illustrated here appears smooth at optical wavelengths, with optical transmittance and reflectance summing up to 100 %, as discussed later on.

Atomic force microscopy (AFM) images (Fig. 3) show the roughness of two-times deposited SnS films of series ZnS/SnS and CdS/SnS. Average roughness (Ra) of the films of series ZnS/SnS is 10.8 nm and for series CdS/SnS is 14.2 nm and root mean square roughness (Rq) is 13.4 and 18.00 nm respectively. Maximum height of the profile (Rt) is 95.4 nm for series ZnS/SnS and 143.2 nm for series CdS/SnS. The observed difference in the surface morphologies of the films on different substrates could result from the difference in the deposition mechanisms of the films on different substrates. The roughness at the film surface is smaller than the optical wavelengths, and the films would behave specular in optical reflectance.

### 3.3 Structural properties

The X-ray diffraction (XRD) patterns of thin films of one, two and three-times deposited films of the series CdS/SnS are shown in Fig. 4. Similar dependence of XRD pattern on the film thickness was noticed for series ZnS/SnS as well. All the major peaks in the PDF card 01-072-8499 for SnS match those of the XRD pattern of the thicker film. The

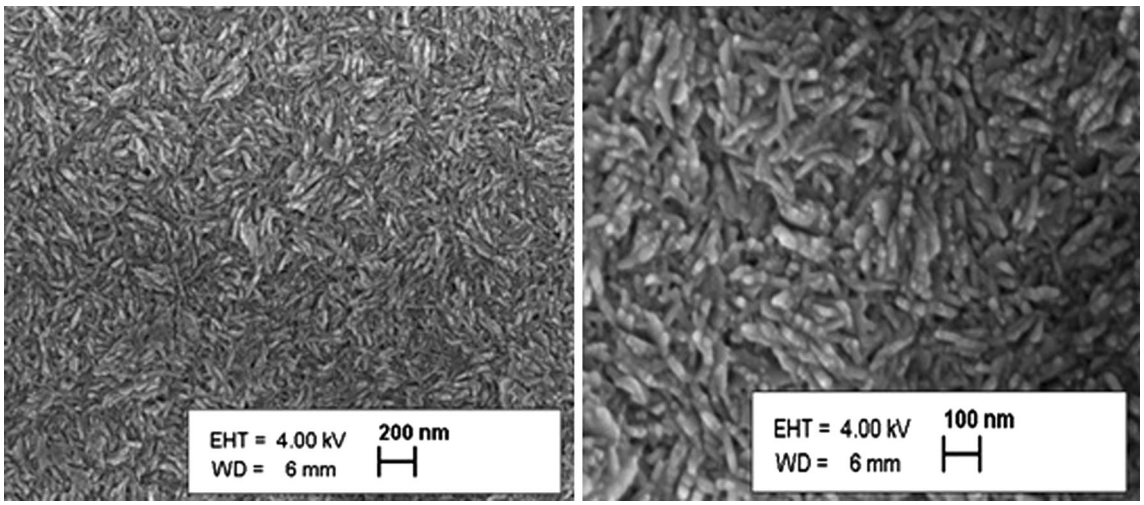


**Fig. 1** SEM images of SnS films of series ZnS/SnS

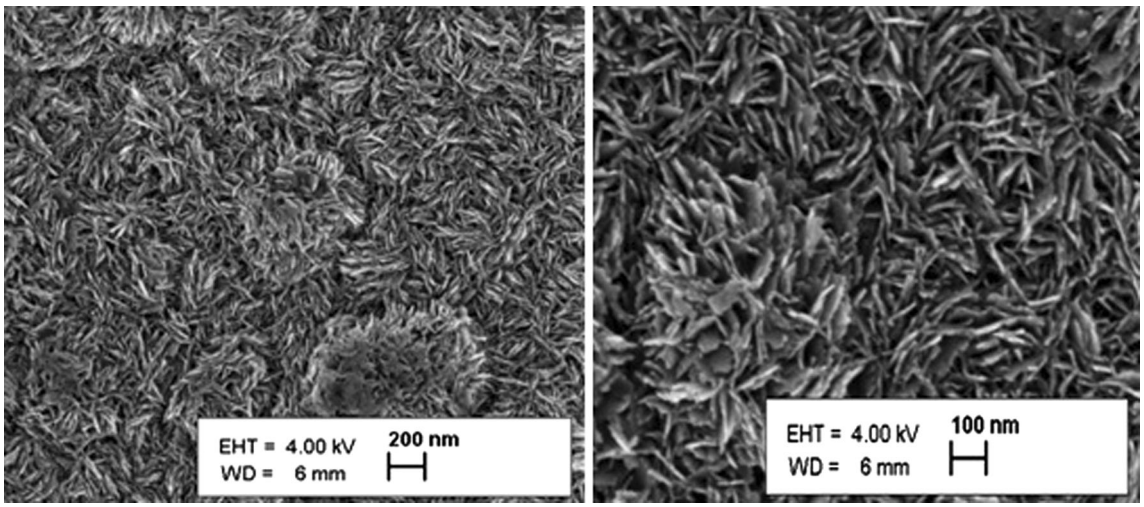


**Fig. 2** SEM images of SnS films of series CdS/SnS

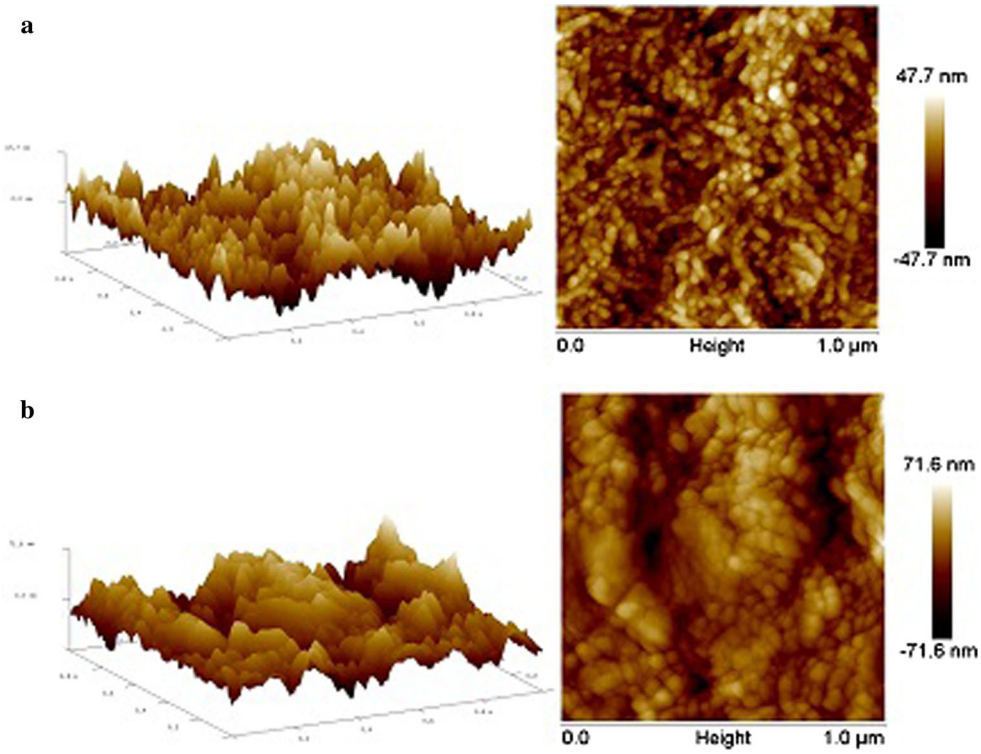


**Fig. 3** AFM images of two-times deposited SnS films on **a** ZnS substrate and **b** CdS substrate

peak at $2\theta = 31.60°$ corresponding to (040) planes; at 26.5° of (120); at 22.6° of (110); at 38.9° of (131); and at 45.3° corresponding to (150) planes of the orthorhombic phase of herzenbergite SnS are all noted. Improvement of crystallinity with the thickness was observed also by other researchers [12]. XRD pattern may contain also some peaks of CdS structure at $2\theta = 26.5°$, 30.6°, 51.1°, 53.1° and 64.1°, but this peaks coincide with SnS peaks. There is no indication of other possible additional phases in the films. All the films exhibit (040) plane as preferred and peak of this plane was used for crystallite size calculations. Crystallite size slightly grows with thickness in both series: from 112 to 130 Å for series ZnS/SnS and from 130 to 161 Å for series CdS/SnS.

Raman analyse was also made to determine more precisely phase composition of films on different substrates. Results of Raman analyse (Fig. 5) were analogical to our XRD results and didn't show the existence of any additional phases in the films, all the peaks in Raman spectra correspond to tin monosulphide phase [13, 14]. On the plot

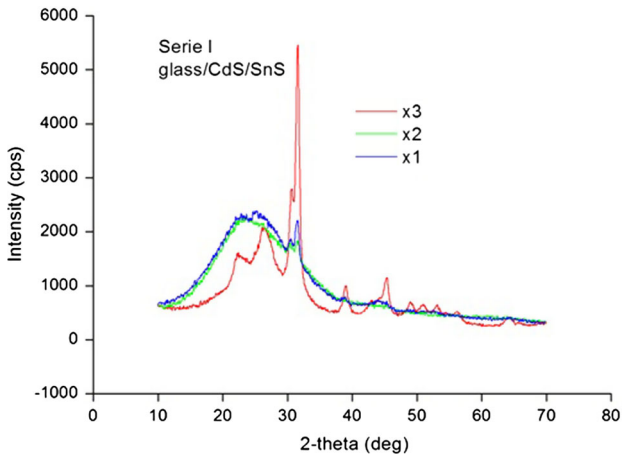


**Fig. 4** XRD patterns of CdS/SnS thin films of one and three-times deposited SnS films of series CdS/SnS

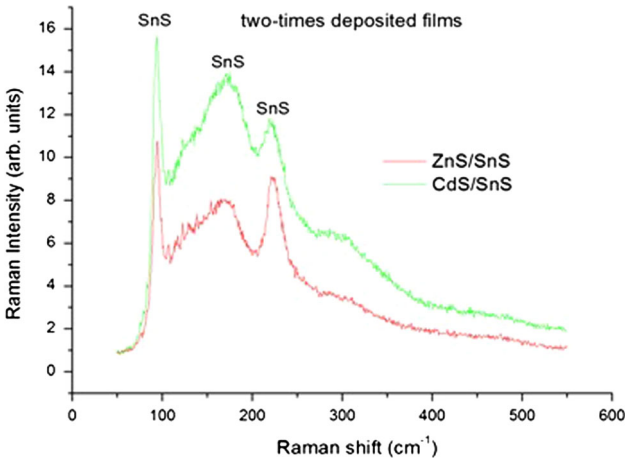


**Fig. 5** Raman spectra of SnS thin films deposited on ZnS and CdS substrates

of CdS/SnS serie can be seen small peak at 306 $cm^{-1}$, which can be attributed to CdS peak (305 $cm^{-1}$). At the same time there is no peak at the same place on the graph of serie ZnS/SnS.

### 3.4 Optical properties

Figure 6 shows the room temperature optical transmittance ($T$) and specular reflectance ($R$) curves of one and three-times deposited SnS films of series (a) ZnS/SnS and (b) CdS/SnS recorded at the wavelength range of 200–2,500 nm. The specular nature of the films is illustrated by T + R of >90 % in general for all the films for large wavelengths, >2,000 nm.

The absorption edge in the transmittance curves fall in the region of 700–900 nm without any bending, which indicates once more to the absence of additional phases

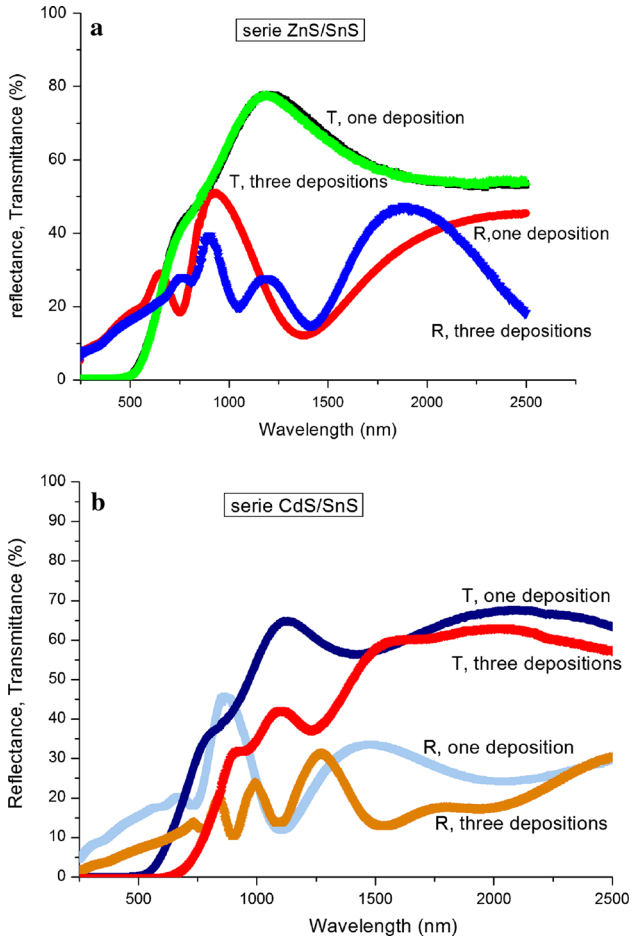


**Fig. 6** Transmittance and reflectance spectra of one and three-times deposited SnS films of series **a** ZnS/SnS and **b** CdS/SnS

presented in material. It can be observed from the Fig. 6 that the absorption edge shifts toward the higher wavelength as the thickness increases with number of depositions in series CdS/SnS. Such tendency was also observed in other works [16].

The optical energy band gap ($E_g$) of the as-grown SnS layers was calculated using the relation, $(\alpha h\nu) = A\ (h\nu - E_g)^n$. Where $\alpha$ is the absorption coefficient, A is a constant, h$\nu$ is the energy of the incident light and n is the nature of transition between the bands in the material.

In the present study, the nature of the transition followed is indirect allowed (n = 2) and the energy band gap can be determined by extrapolating the straight line portion of the curve $(\alpha h\nu)^{1/2}$ versus $h\nu$ on the energy axis. Band gap values decrease with number of deposition from 1.49 to 1.39 eV for films deposited on ZnS substrate and from 1.5 to 1.28 eV for films deposited on CdS substrate. This decrease could be attributed to the grain size dependency of band gap [10]. Such tendency was also observed by Ghosh et al. [15].

The $E_g$ of the CdS/SnS thin film (1.28 eV) is close to that of orthorhombic SnS (1.3 eV) as determined from photoreflection measurements.

Hot-probe method was used to determine type of conductivity of the SnS films and all the layers showed p-type conductivity. Films of both series have very high resistivity: 120 MΩ for three-times deposited films of series CdS/SnS and 130 MΩ for three-time deposited films of series ZnS/SnS. Resistivity increases with decreasing films thickness. Further experiments are needed to decrease it.

## 4 Conclusions

Films have the structure of orthorhombic herzenbergite tin monosulphide with stoichiometric composition and good pin-hole free surface morphology of rod (ZnS substrate) or flake (CdS substrate) shape of the particles. XRD, Raman and EDX analyses didn't show any additional phases in the films. Crystallinity of the as-deposited films improves in multiple deposition process and three times deposited films have well-determined crystalline structure. Grain sizes slightly grow in multiple deposition process of films. Band gap decreases with the thickness of the films and for three-times deposited it is equal to 1.28 eV. Films on both substrates have very high electro resistivity which should be improved with further chemical and thermal treatments.

**Acknowledgments** The authors are grateful to Patricia Altuzar for the XRD measurements, Jose Campos for the SEM-compositional analyses and photoconductivity response measurement, Oscar Gomez Daza for the optical measurements, all of them at the *Instituto de Energias Renovables—UNAM*. We acknowledge the use of experimental facility of CONACYT-Mexico project 123122-LIFYCS. Estonian Centre of Excellence in Research Project TK117T "High-technology Materials for Sustainable Development", Estonian Energy Technology program (project AR 10128), Estonian Ministry of Higher Education and Science (targeted project T099) and Estonian Science Foundation (MJD213, G8147) are acknowledged for the financing of the research.

## References

1. G.E. Yan-hui, G.U.O. Yu-ying, S.H.I. Wei-min, Q.I.U. Yong-hua, W.E.I. Guang-pu, J. Shanghai Univ. (Engl. Ed.) **11**(4), 403–406 (2007)
2. E. Guneri, F. Gode, C. Ulutas, F. Kirmizigul, G. Altindemir, C. Gumus, Chalcogenide Lett. **7**(12), 685–694 (2010)
3. G. Hodes, *Chemical Solution Deposition of Semiconductor Films* (Marcel Dekker Inc., New York, 2002)
4. S. Aksaya, T. Ozer, M. Zor, J. Appl. Phys. **47**, 30502 (2009)
5. P. Sinsermsuksakul, K. Hartman, S.B. Kim, J. Heo, L. Sun, H.H. Park, R. Chakraborty, T. Buonassisi, R.G. Gordon, Appl. Phys. Lett. **102**, 053901 (2013)
6. W. Wu, W. Shi, Z. Hu, S. Liu, W. Yang, G. Wei, in *Proceedings of SPIE 7995, Seventh International Conference on Thin Film Physics and Applications*, (February 17, 2011), 79952D
7. O.L. Arenas, M.T.S. Nair, P.K. Nair, Semicond. Sci. Technol. **12**, 1323 (1997)
8. M.T.S. Nair, J. Appl. Phys. **75**(3), 1557–1564 (1994)
9. P.P. Hankare, A.V. Jadhav, P.A. Chate, K.C. Rathod, P.A. Chavan, S.A. Ingole, J. Alloys Compd. **463**, 581–584 (2008)
10. T.H. Patel, Open Surf. Sci. J. **4**, 6–13 (2012)
11. Y. Wang, Y. BharathKumar Reddy, H. Gong, J. Electrochem. Soc. **156**(3), H157–H160 (2009)
12. A. Akkari, C. Guasch, N. Kamoun-Turki, J. Alloys Compd. **490**, 180–183 (2010)
13. L.S. Price, I.P. Parkin, A.M.E. Hardy, R.J.H. Clark, Chem. Mater. **11**, 1792–1799 (1999)
14. S. Kodigala, *Thin Film Solar Cells From Earth Abundant Materials: Growth and Characterization of $Cu_2(ZnSn)(SSe)_4$ Thin Films and Their Solar Cells* (Elsevier Inc., London, 2014), p. 26
15. B. Ghosh, R. Bhattacharjee, P. Banerjee, S. Das, Appl. Surf. Sci. **257**, 3670 (2011)
16. A.-H.K. Elttayef, H.M. Ajeel, A.I. Khudiar, J. Mater. Res. Technol. **2**, 182–187 (2013)